RESEARCH ARTICLE

Muscle fatigue assessment through energy analysis of fused inertial and electromyographic signals

Guangcai Zhang[1, *], Shiwen Zhang[2], Xiaoguang Wu[2]

[1]College of Intelligent Equipment, Suzhou Vocational Institute of Industrial Technology, Suzhou, Jiangsu, China. [2]School of Electrical Engineering, Yanshan University, Qinhuangdao, Hebei, China.

Received: January 28, 2026; **accepted:** May 18, 2026.

Exercise-induced deep muscle fatigue compromises motor function and increases the risk of muscular injury. This study investigated the correlation between metabolic dynamics during muscle contraction and the onset of muscle fatigue. Utilizing arm dumbbell curls as an experimental model, real-time electromyographic and inertial signals were fused to analyze fatigue from a macroscopic energy output perspective. The dynamic time warping (DTW) algorithm was employed to identify the critical threshold of deep muscle fatigue by analyzing angular velocity signals of forearm motion. Muscle energy output at the deep fatigue threshold was calculated using the Hill model, determining its ratio relative to the muscle's maximum energy capacity. Results indicated that muscles entered a state of deep fatigue at 72.78 ± 2.70% of their maximum energy output. Furthermore, the energy expenditure across various fatigue levels up to this critical point provided a quantifiable basis for assessing recovery during rest periods. Experimental data demonstrated that, after 120 s rest provided, muscle energy recovery reached 41.707 ± 1.875% of the maximum output. Based on the analysis of energy output and recovery, a quantitative framework was formulated to determine appropriate repetitions for dumbbell curls under fixed load and movement frequency. This approach effectively prevented deep muscle fatigue by utilizing muscle energy output proportions to inform both exercise execution and recovery strategy design.

Keywords: muscle fatigue; inertial signals; surface electromyography; dynamic time warping; energy output.

[*]**Corresponding author:** Guangcai Zhang, College of Intelligent Equipment, Suzhou Vocational Institute of Industrial Technology, Suzhou, Jiangsu 215000, China. Email: zhangguangcai_siit@163.com.

Introduction

Muscle contraction leads to reduced strength and fatigue. When the strength reaches the support threshold, the contraction performance falls into deep fatigue. Accurate detection and assessment of muscle fatigue are essential for preventing deep fatigue and injury [1]. Effective fatigue monitoring and management at this stage are necessary. Methods for measuring muscle fatigue during exercise can be classified into subjective and objective measurements. Subjective measurements depend on an individual's perception of fatigue and are commonly assessed using the ratings of perceived exertion (RPE) scale, ranging from 6 to 20 [2]. Although this method is inexpensive and minimally disruptive to the exercise process, its accuracy is limited by the multidimensional nature and delayed perception of fatigue, as well as individual variability in fatigue perception [3]. Objective measurement methods assess human fatigue by analyzing the relationship between physiological signals and muscle fatigue. This method eliminates variability caused by individual perception and delivers real-time, objective assessments of muscle fatigue.

Surface electromyography (sEMG) is frequently used as a physiological signal to estimate muscle fatigue. Studies have shown that the time-domain characteristics of sEMG generally increase as muscle fatigue develops [4]. In contrast, the mean and median frequencies in sEMG frequency-domain analysis typically decrease with increasing fatigue [5]. Moreover, the multiscale entropy method, which leverages the nonlinear and multi-timescale properties of sEMG, can effectively characterize the muscle fatigue process [6]. However, sEMG-based fatigue detection methods still lack accuracy due to signal interference and the physiological complexity of participants. Inertial signals accurately reflect changes in muscle performance by capturing the spatial position of limbs during movement [7]. Ameli *et al*. applied the dynamic time warping (DTW) algorithm to compare motor postures pre- and post-fatigue, using the magnitude of difference as an indicator of fatigue degree [8]. However, this method can only distinguish between pre- and post-fatigue phases and cannot predict or analyze muscle fatigue. Recently, research has focused on multi-source information fusion approaches to provide more comprehensive, accurate, and individualized muscle fatigue assessments. This approach integrates multi-dimensional activity data to comprehensively assess muscle fatigue during exercise [9]. Ai *et al*. combined sEMG and inertial signal analysis to explore differences between fatigued and non-fatigued phases [10]. Most signal analysis methods only carry out basic joint analysis of multiple signals and do not deeply integrate physiological signals. The methods of estimating muscle fatigue relying on real-time physiological signals often lack the whole process analysis of exercise, which ignores the overall process analysis of exercise relying on instantaneous detection data. Physiological signals are easily affected by external factors and restricted by the complex physiological mechanisms of the human body, which make it complicated to use physiological signal analysis methods for real-time and accurate muscle state assessment and prediction. Therefore, developing a method for assessing muscle condition that combines both quantitative and predictive capabilities, enabling the rational planning and real-time monitoring of fitness training, has become a critical issue that urgently needs to be addressed in this field. From a cellular and microscopic perspective, ATP catabolism during the high energy demand of muscle contraction increases the concentrations of creatine (Cr) and inorganic phosphate (Pi) [11]. The elevated Pi content is believed to inhibit the sarcoplasmic calcium release channel and contribute to the precipitation of Ca^{2+}-Pi, a calcium-containing complexes, in sarcoplasmic vesicles, reducing the amount of releasable Ca^{2+} and ultimately inhibiting muscle force generation [12]. Additionally, ATP catabolism releases hydrogen ions, reducing intracellular pH, which inhibits maximal muscle contraction force, thereby impairing muscle performance and increasing fatigue [13]. Changes in sEMG are attributed to a gradual slowing of muscle fiber conduction velocity caused by alterations in intracellular substance concentrations [14]. During the resting phase after contraction, intracellular substance concentrations recover through feedback regulation with Pi and hydrogen ion levels gradually returning to normal, alleviating muscle fatigue [15].

The purpose of this research was to improve the accuracy of muscle fatigue detection and prediction and help optimize the arrangement of muscle contraction. The study adopted a physiological approach to quantify and predict muscle status by calculating changes in muscle energy during exercise utilizing the principle of sEMG to detect muscle fatigue according to the changes in the concentration of metabolites during muscle contraction and rest. In the simplified model of the dumbbell curl exercise, muscle work and recovery were represented as battery discharge and recharge processes, respectively. In the “discharge” phase, the muscle released energy. When the muscle strength was reduced to the point that it was difficult to bear the load, the movement was deformed, and fatigue occurred. After resting, muscles entered the "charging" state to restore strength. By calculating changes in muscle energy during exercise and recovery phases, this study extended muscle fatigue prediction to interval training scenarios, enabling continuous tracking of muscle fatigue progression. Based on these predictions, a dumbbell curl exercise plan that effectively balanced exercise efficiency and safety was developed, thereby providing a systematic theoretical foundation and technical support for exercise planning.

Materials and methods

Participants and data acquisition

A total of 12 non-professional male volunteers with little fitness experience, a mean age of 24 ± 2 years, a mean height of 173.2 ± 4.3 cm, and a mean weight of 76.5 ± 4.15 kg were involved in this study. The mean body mass index (BMI) for all participants was 21.25 ± 2.75. Participants were required to avoid strenuous exercise and physical and mental fatigue 12 hours before the experiment. All procedures of this study were approved by the Ethics Committee of Yanshan University (Qinhuangdao, Hebei, China). Informed consent was signed by all participants before the experiment. To acquire sEMG and inertial signal data, a custom wireless, real-time, wearable sEMG-inertial data acquisition device was developed in house, which synchronously acquired and fused the sEMG and inertial signals of the forearm during movement. The device was divided into 5 parts including sEMG acquisition unit, inertial signal acquisition unit, microcontroller unit, power supply circuit unit, and data transmission unit. After the warm-up, the signal acquisition equipment was placed at the midpoint of the participant's right forearm and Ag-AGCl disposable electrodes (Shanghai JunKang Medical Equipment Limited Company. Shanghai, China) were attached at 2 cm intervals on the biceps. During the experiment, the experimenter monitored the participants and took measures to ensure their safety.

Acquisition of maximum voluntary muscle contraction signals

The participants held the right forearm with the left hand and maintained the optimal muscle fiber length. After receiving the instruction, they applied maximum force to the body direction with the right arm, and the left hand simultaneously gave a reaction force to generate maximum muscle force. The maximum muscle activation was measured by sEMG when the elbow joint had maximum free contraction, while the muscle activation ratio was quantified.

Acquisition of the cycle number of the maximum muscle contraction

An exercise cycle was defined as the elbow movement of dumbbell curl starting from a natural hanging state, bending to the target position, and then returning to the starting position. Participants performed dumbbell curls with 7 kg, bent to 90° in the first round, and instructed to maintain a consistent movement frequency during the exercise and strictly adhere to the specified bending angle with each period separated by 2 seconds. The experimental process was conducted with continuous monitoring and was immediately terminated once the participant failed to a cycle. After a 24-hour interval, the second round started bending to 140°. The participants were urged to exert their full strength until exhaustion to determine the maximum number of cycles.

Acquisition of signals of a fixed number of bends

Based on the 90° dumbbell curl standard established above, the participants completed 20 cycles for each set and 5 sets in total with a rest interval of 120 seconds between sets. During the rest, the arms hung naturally in a still state. One set was ended if the participant was unable to complete one cycle in that set. The next set would start after 120 seconds of rest until 5 sets were completed. The same procedures were repeated when dumbbell curl angle was changed to 140°.

sEMG data pre-processing

sEMG signal filtering was performed by using a multiple feedback circuit filter with Butterworth response. The high-pass cut-off frequency of the sEMG modulation circuit was set as 5 Hz, and the theoretically cut-off frequency range of the designed sEMG circuit was between 5 Hz and 497.6 Hz. A second-order notch filter was used to suppress the 50 Hz frequency interference.

Kinetic modeling of muscle activation

Muscle activation is a critical parameter for calculating muscle energy output, representing the muscle's response level to neural stimulation. sEMG reflects motor intention and provides information about muscle nerve activation and contraction. Thus, sEMG can be converted into muscle activation levels using a muscle activation kinetic model [16]. Electromyography measures the electrical activity of muscles. Muscle activation can trigger the generation of force. However, a time lag exists between changes in charge distribution and the exertion of muscle force, resulting in the phenomenon of "delayed activation". A second-order differential equation characterizing the kinetics of the excitation reflected the time delay phenomenon in the process of charge change until muscle force production as follows.

$$u(t) = M\frac{de^2(t)}{dt^2} + B\frac{de(t)}{dt} + Ke(t) \tag{1}$$

where $e(t)$ was the filtered sEMG signal. $u(t)$ was the degree of neural activity. *M*, *B*, *K* were constants. For discrete signal acquisition of sEMG, the discrete equation of backward difference could be used to represent the above equation as below.

$$u(t) = \alpha e(t-d) - \beta_1 u(t-1) - \beta_2 u(t-2) \tag{2}$$

where the coefficients α, β_1, β_2 were defined as the second-order differential equation. *d* was the delay factor of sEMG. Through this equation, the sEMG value $e(t)$ was mapped to the neural activity value $u(t)$. For simplicity of calculation, this study used a single-parameter exponential model to describe the muscle activation kinetics [17]. The muscle activation model including a linear and a nonlinear component were determined by a single parameter and calculated below.

$$a(t) = \frac{e^{Au(t)} - 1}{e^A - 1} \tag{3}$$

where $a(t)$ was the degree of muscle activation. *A* was a nonlinear shape factor with a value range [-3, 0]. When *A* = 3, it indicated a highly exponential relationship, while A = 0 indicated a complete linear relationship.

Dynamic time warping

Dynamic time warping (DTW) adjusted the alignment of two time series of different lengths in a dynamic way to achieve the optimal alignment between the elements [18]. If there were two time series $X = \{x_1, x_2, x_3 \dots x_n\}$ and $Y = \{y_1, y_2, y_3 \dots y_m\}$ with lengths n and m respectively, there existed an alignment π that described the alignment of each element in the two time series as follows [19].

$$\pi = \{(\pi_1^X, \pi_1^Y), (\pi_2^X, \pi_2^Y), \text{K}, (\pi_k^X, \pi_k^Y), \text{K}\ (\pi_K^X, \pi_K^Y)\} \tag{4}$$

where π was a set of *K* binary tuples. Each binary tuple contained two elements, which represented the position information of some elements in the two time series *X* and *Y*, respectively. To ensure smooth matching paths and continuously match similar segments, the paths needed to be continuous, and the matching order was monotonic. All the aligned paths that met the constraints were represented as *W*. The similarity of the two times series was measured by the minimum value of the sum of the distances between the corresponding points along all the aligned paths as shown below.

$$DTW(X,Y) = \min_{\pi \in W} \sum\nolimits_{(i,j)\in\pi} dis(x_i, y_j) \tag{5}$$

The Euclidean distance calculation function was used to calculate the distance between two time series points as illustrated below.

$$dis(x_i, y_j) = \left\| x_i - y_j \right\| \tag{6}$$

Based on this method, a $n \times m$ cost matrix M was constructed and could be transformed to solve the problem of the X and Y subsequences through the recursive way below.

$$DTW(X_i, Y_j) = dis(x_i, y_j) + \min \begin{cases} DTW(X_{i-1}, Y_j) \\ DTW(X_{i-1}, Y_{j-1}) \\ DTW(X_i, Y_{j-1}) \end{cases} \tag{7}$$

where X_i was the subsequence of the X sequence starting at l and ending at i. Y_j was the subsequence of the Y sequence starting at 1 and ending at j. The last element, $M(m,n)$, of the cost matrix M was the DTW distance, calculated based on the fluctuation trend of the sequence [20].

Muscle fatigue analysis using dynamic time warping methods

To minimize the impact of movement differences of subjects on the experimental results, this study took the angular velocity signal of each subject in the non-deep fatigued state as the comparison benchmark of the DTW algorithm. In the dumbbell curl experiment, the Borg rating of perceived exertion test was used to evaluate the perceived effort of participants. The angular velocity signal of the movement cycle with the perceived effort in the range of 6 to 12 was selected as the benchmark. The benchmark signal was compared with the angular velocity signals of all movement cycles through the DTW similarity to quantify muscle fatigue. There were m_d periods in the motion and n_d periods in the benchmark signal. ω_i was the angular velocity signal of the $i-th$ period. $\Omega_m = \{\omega_1, \omega_2 \ldots \omega_{n_d}, \ldots, \omega_{m_d}\}$ represented the set of angular velocities of all periods, and $\Omega_n = \{\omega_1, \omega_2, \ldots, \omega_{n_d}\}$ represented the set of benchmark angular velocities. The angular velocity signals of m_d sets were used as the test signals. The test signals were calculated for DTW similarity, respectively, with the n_d sets of benchmark angular velocity signals. The calculated DTW distances thus constituted a DTW similarity comparison matrix $DTW_{m \times n}$ with respect to benchmark signals as follows.

$$DTW_{m_d \times n_d} = \begin{bmatrix} DTW(\omega_1, \omega_1) & DTW(\omega_1, \omega_2) & \cdots & DTW(\omega_1, \omega_{n_d}) \\ DTW(\omega_2, \omega_1) & DTW(\omega_2, \omega_2) & \cdots & DTW(\omega_2, \omega_{n_d}) \\ \vdots & \vdots & \ddots & \vdots \\ DTW(\omega_{m_d}, \omega_1) & DTW(\omega_{m_d}, \omega_2) & \cdots & DTW(\omega_{m_d}, \omega_{n_d}) \end{bmatrix} \tag{8}$$

The similarity $\alpha_\omega(j)$ between the angular velocity of the *i*-th period and the benchmark angular velocity signal was the mean value of the matrix *i*-th rows.

$$\alpha_\omega(j) = \sum_{i=1}^{n_d} \frac{DTW_\omega(\omega_j, \omega_i)}{n_d} \tag{9}$$

Hill model energetic properties

The Hill model rooted in the ultrastructure of muscles simplified muscle representation into three components including contractile elements (CE), parallel elastic elements (PEE), and series elastic elements (SEE) [21] (Figure 1). The CE generated active contraction force in the muscle, corresponding to contractile tissue such as muscle proteins within muscle fibers. The PEE referred to non-contractile tissue within the muscle that generated passive tension when stretched such as structural proteins and extracellular connective tissue. The SEE represented the elastic tendon tissue connecting the muscle to the skeleton. The interaction among these elements explained the process of muscle contraction and relaxation [22]. This study utilized a muscle energy consumption mathematical model to estimate the metabolic energy consumption in muscle fiber tissue from the micro perspective of ATP catabolism during the dumbbell biceps exercise. The model was established based on a single isolated muscle metabolism experiment [23]. The metabolic energy consumption of centripetal contraction, isometric contraction, and centrifugal

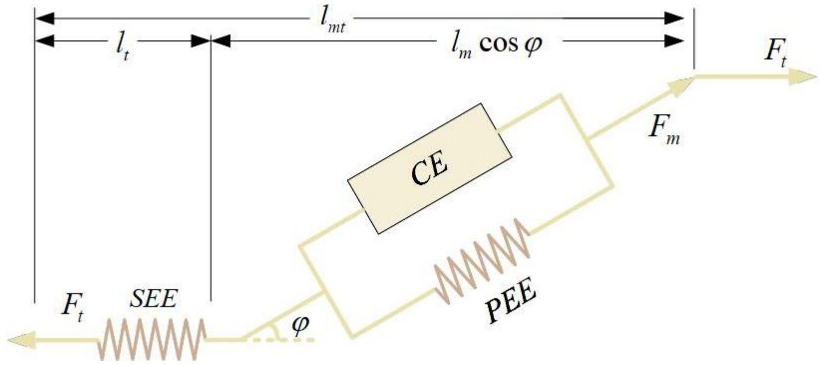

Figure 1. Representation of muscle ultrastructure and the Hill model.

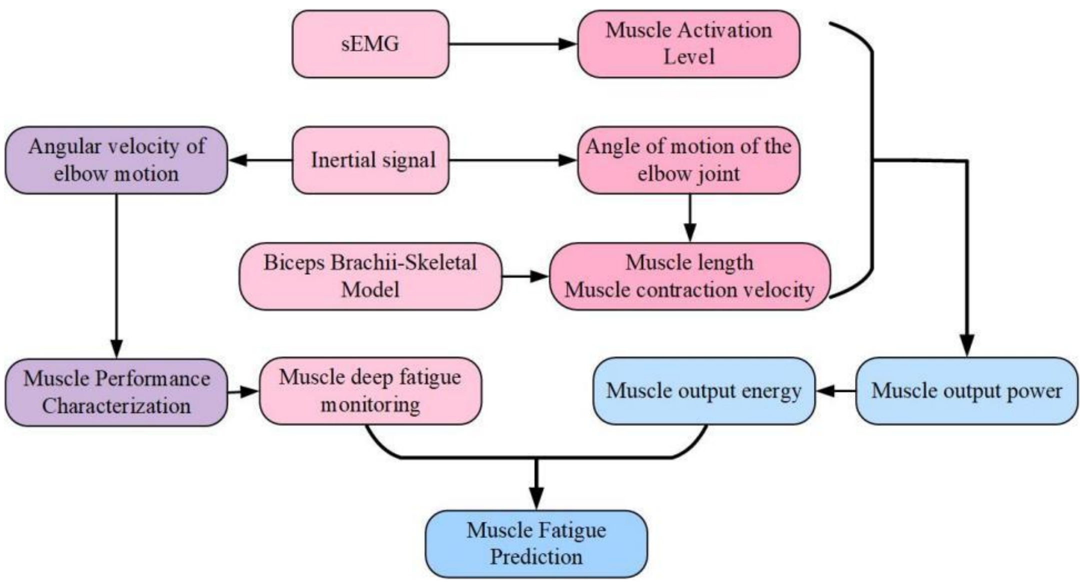

Figure 2. Framework of muscle deep fatigue prediction method.

contraction were calculated using this model as follows.

$$P_{Met} = a \cdot F_{\max} \cdot v_{\max} \cdot f_{Met}(\tilde{v}_m) \tag{10}$$

where the degree of muscle activation was represented by a. The maximum force during the muscle isometric contraction represented by F_{max}. The maximum contraction velocity of muscle fibers was represented by v_{max}, which related to the optimal muscle fiber length l_{o}^{m}. This study adopted the value of $10l_{o}^{m}$ cm/s based on relevant literature [24]. $\tilde{v}_m$ was the normalized muscle fiber contraction velocity. A normalized correlation function of the contraction velocity of normal muscle fibers was shown as follows.

$$\begin{cases} f_{Met}(\tilde{v}_m) = 0.23 - 0.16e^{-8\tilde{v}_m} & \tilde{v}_m \geq 0 \\ f_{Met}(\tilde{v}_m) = 0.01 - 0.11\tilde{v}_m + 0.06e^{23\tilde{v}_m} & \tilde{v}_m < 0 \end{cases} \tag{11}$$

Then, the muscle metabolic energy output was calculated through the Hill model's energetic characteristics from 0 to t_0 during the exercise and was expressed as below.

$$W_{Met} = \int_0^{t_0} P_{Met}(t)dt \tag{12}$$

Normalization of energy calculation

To accurately describe the muscle energy output during the exercise and exclude the influence of the unknown parameters to be optimized on the energy calculation, the maximum muscle output energy during the curl exercise with 7 kg dumbbell was used as the research reference. The characterization of specified load movement was shown below.

$$p = \frac{\int_0^{t_1} P_{Met}(t)dt}{\int_0^{t_2} P_{Met}(t)dt} \times 100\% \qquad (13)$$

where p was the proportion of the energy proportion of a certain exercise stage with duration t_1 to the total energy of total exercise with duration t_2. Integrating with the above analysis methods, this study developed a muscle fatigue prediction method based on energy information analysis using the fusion of inertial and sEMG signal data (Figure 2).

Results and discussion

Muscle activation calculation

The biceps muscle activation during a single dumbbell curl exercise showed that muscle activation was low in the early phase of the exercise when the elbow joint remained extended and the arm hung naturally to support the dumbbell. The muscles were then rapidly activated and generated contractile force and actively contracted, converting energy into kinetic energy, controlling the elbow joint to perform internal rotation with the dumbbell against inertia. In the next phase, the degree of muscle activation gradually decreased, the muscle stretched, and the elbow joint was controlled to perform external rotation movement with the dumbbell (Figure 3). Meanwhile, a certain muscle tension was maintained to resist the gravity of the dumbbell to ensure the stability of the curl movement. In the dumbbell curl exercise, the degree of muscle activation reflected the muscle's exertion and provided data support for the subsequent calculation of muscle energy expenditure.

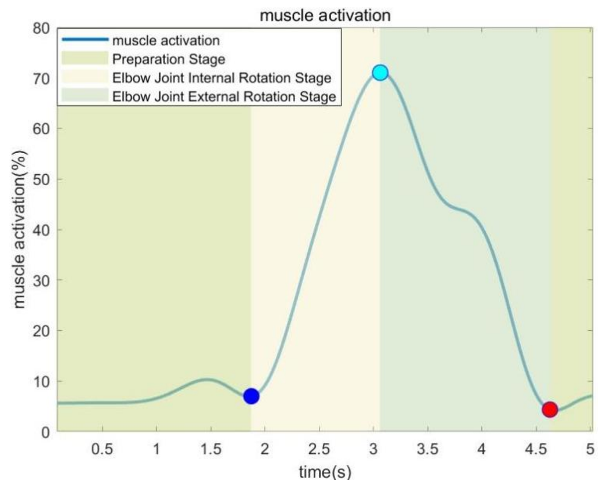

Figure 3. Biceps brachii muscle activation.

Muscle fatigue discrimination based on DTW

The angular velocity signals of each participant were measured during the dumbbell curl, and participant 1 was selected for analysis. The participant performed 36 dumbbell curls. The angular velocity signals of the 1st, 18th, and 35th repetitions showed that, during the first half cycle of the signal, the muscle contraction drove the elbow joint to perform internal rotation, and the elbow joint drove the dumbbell to overcome gravity and lift upward. During the second half, the muscle relaxed, while elbow joint performed external rotation, and the dumbbell descended smoothly (Figure 4). Analysis showed that the angular velocity signals of the 1st and 18th cycles were similar, while the first half of the 35th cycle was lower and the second half was slightly higher, which indicated that the ability of the muscles in the 35th cycle to overcome gravity and maintain stability became weaker, resulting in a decline in performance [25]. Prolonged muscle contraction might exacerbate fatigue, leading to significant changes in angular velocity signals, and allow for the detection of a critical point for identifying deep muscle fatigue. To quantify changes in angular velocity signals, DTW algorithm was applied to analyze the muscle

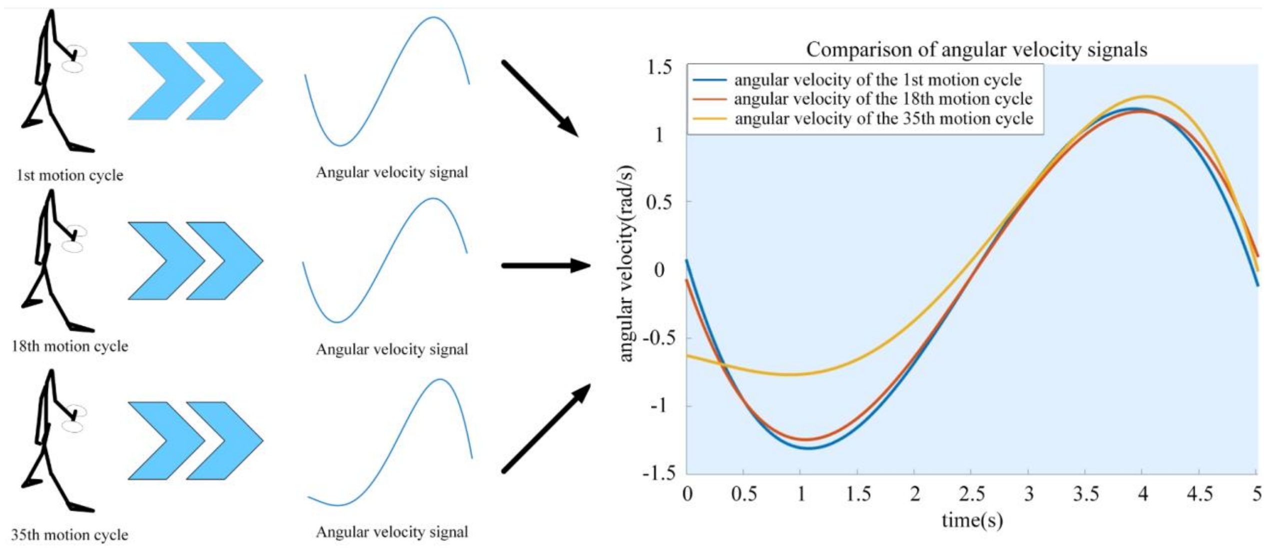

Figure 4. Angular velocity during movement.

fatigue status of each movement cycle. To ensure the generalizability of the analysis and reduce the impact of outliers on the trend, the least square polynomial fitting method was used to process the results of the fatigue analysis. The result demonstrated that DTW distance values between each angular velocity signal and the benchmark signal in the early stage of movement remained stable and were all lower than 5. The mid-stage posture was roughly similar to the benchmark. The DTW distance values in later stage between the angular velocity signal and the benchmark signal rose sharply, and all of them exceeded 5, indicating that there were significant differences between the later posture and the benchmark (Figure 5). Further analysis indicated that, when the DTW distance values were low or stable, the muscle was not deeply fatigued. The maximum contraction force was accompanied by a decrease in consumption, but the muscle could still maintain a good state under the current load. The DTW distance values rose relatively fast, and muscle entered a deep fatigue state. The maximum muscle contraction force was below the critical level of sports performance, the sports performance was reduced significantly, and it was easy to get injured.

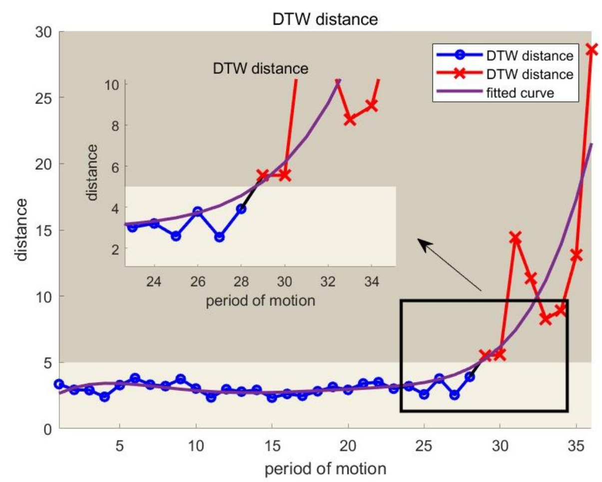

Figure 5. Results of DTW fatigue analysis.

Muscle depth fatigue discrimination based on energy output

Using the energy properties of the Hill model and combining with the previous calculation method of muscle activation, the inertial signals and sEMG were analyzed to estimate the muscle energy output of dumbbell curls. The muscle deep fatigue criterion based on DTW algorithm was then used to calculate the ratio of energy output between the deep fatigue stage and the non-deep fatigue stage to explore the relationship between this ratio and deep fatigue. The variations of muscle output power in the

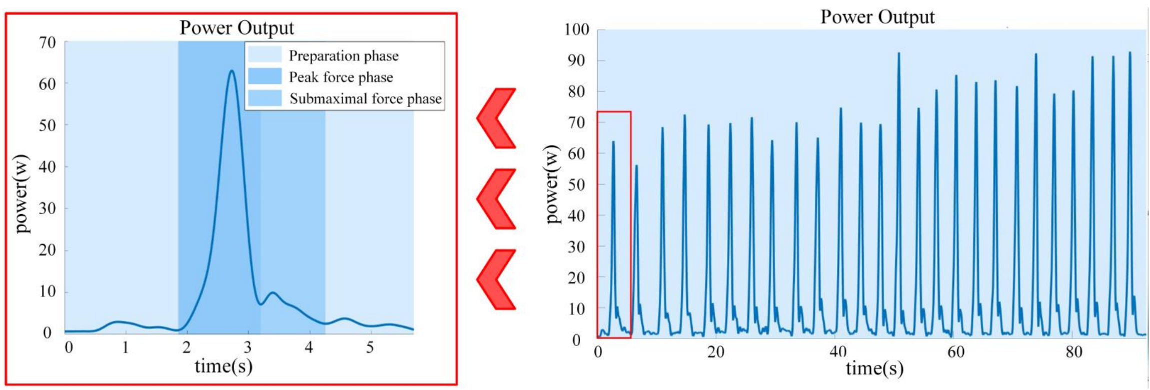

Figure 6. Power output during exercise.

dumbbell curl exercise at 90° showed that, when muscle fatigue increased, the muscle output power of repeated movements in the later stage was usually higher than that of repeated movements in the early stage with low fatigue. However, the complex physiological process made this increase unstable (Figure 6). Sometimes, the output power in the case of deep fatigue was even lower than that in the state of less fatigue. Therefore, simply focusing on the characteristics of a single cycle in muscle fatigue analysis might not be able to accurately reflect the muscle state. This study comprehensively analyzed the muscle movement throughout the process to accurately evaluate the depth of muscle fatigue. The energy output during dumbbell curl exercises at 90° and 140° demonstrated that, despite being in different cycles, the maximum muscle energy output was approximately consistent under the same muscle load at dumbbell curl exercise of 90°and 140°. The results of the maximum muscle energy output ratios for all participants during 90° and 140° dumbbell curl movements indicated that, under the same muscle load, the total muscle energy output ratios calculated using the Hill model were close to 1 (0.9884 ± 0.0593), which suggested that the muscle energy output was consistent (Figure 7). Thus, the total muscle energy output was defined as the maximum muscle energy output, representing participants' muscle movement ability during dumbbell curl exercises to failure under the current load. The maximum muscle energy output at a 90° elbow flexion angle was used as a reference point, describing energy output during muscle movement as a proportion relative to this reference. Additionally, assuming the maximum muscle energy output remained constant under the same load, this study analogized maximum energy output at a 90° elbow flexion angle to the maximum stored energy of a battery, providing data for subsequent energy-based muscle fatigue analysis. According to the DTW muscle fatigue criteria, analysis of the 90° dumbbell curl exercise indicated that cycles 1 - 28 corresponded to the non-deep fatigue stage, while cycles 29 - 36 represented the deep fatigue stage. Thus, the energy expenditure proportion during the non-deep fatigue stage was calculated as follows.

$$p_{\pi/2} = \frac{\int_{NF} P_{Met}(t)dt}{\int_{NF\cup F} P_{Met}(t)dt} \times 100\% \qquad (14)$$

where NF was the non-deep fatigue stage during exercise. F was the deep fatigue stage during exercise. The proportion of energy output during the non-deep fatigue stage was then calculated for each participant with the average value across all participants as 73.277 ± 1.846%. The standard deviation (σ) and mean (μ) were used to calculate the coefficient of variation (CV) as below.

$$CV_p = (\sigma / \mu) \times 100\% \qquad (15)$$

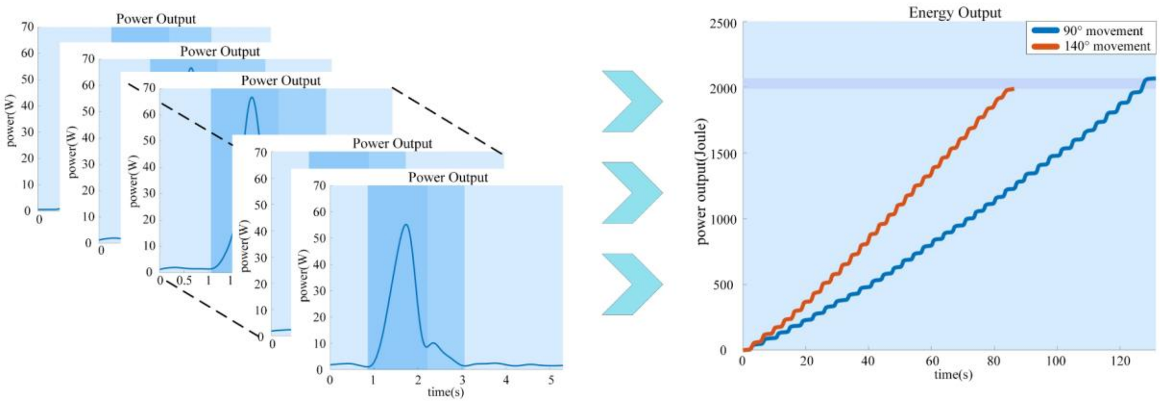

Figure 7. Comparison of Energy Output at Elbow Flexion Angles of 90° and 140°.

The CV for the energy expenditure ratio during the non-deep fatigue stage across all participants was 2.52%. The data was consistent across all participants. Therefore, for non-professional fitness enthusiasts using a 7 kg dumbbell load, when the energy output of the biceps brachii was approximately 72.78 ± 2.70% of the maximum muscle energy output, the maximum muscle strength decreased to a critical level sufficient to maintain adequate performance. At this point, participants were unable to perform standard dumbbell curl exercises, indicating that the muscles had entered a phase of deep fatigue.

Assessing muscle energy recovery status

The DTW muscle fatigue analysis of the dumbbell curl exercise with 120 s of rest between groups showed that, although there was a fixed rest of 120 s between sets, the different muscle fatigue levels at the end of each set made the fatigue gradually increase at the beginning of the next set and the number of repetitions decrease in a non-deep fatigue state. During the 4th and 5th sets, the subject could not complete 20 dumbbell curls, which indicated that the planning of each set of exercise cycles was inadequate and would disrupt the continuity of exercise, reduce efficiency, and increase the risk of muscle injury [26] (Figure 8). The scientific periodization of exercise cycles was critical for optimizing the efficacy of fitness training. Such planning necessitated the integration of individual maximal repetition performance in dumbbell curls with muscular recovery status, which encompassed both peak muscular energy output and regenerative capacity during rest intervals. This investigation centered on elucidating the mechanisms of energy recovery under states of profound muscular fatigue induced by resistance training with the objective of delineating differences in recovery dynamics across varying fatigue intensities. Particular emphasis was placed on characterizing the transition from moderate to profound fatigue phases, which was demarcated as a pivotal focal point within the research framework. The study calculated energy expenditure during the transition from the current set's deep fatigue point to the next set's deep fatigue point after 120 s of rest, which served as an indicator to evaluate total muscle recovery within 120 s as follows.

$$W_r = W_{NF}(i+1) + W_F(i) \tag{16}$$

where the energy recovery amount W_r for the $i-th$ set within 120 s equaled the sum of the non-deep fatigue stage energy output $W_{NF}(i+1)$ of the $i+1$ set and the deep fatigue stage energy output $W_F(i)$ of the $i-th$ set. Since there was no fatigue in the first group, *i* equaled 2, 3, 4. The energy recovery ratio Q_i for the $i-th$ set was calculated as follows.

$$Q_i = \frac{W_r}{\int_{NF \cup F} P_{Met}(t)dt} \times 100\% \tag{17}$$

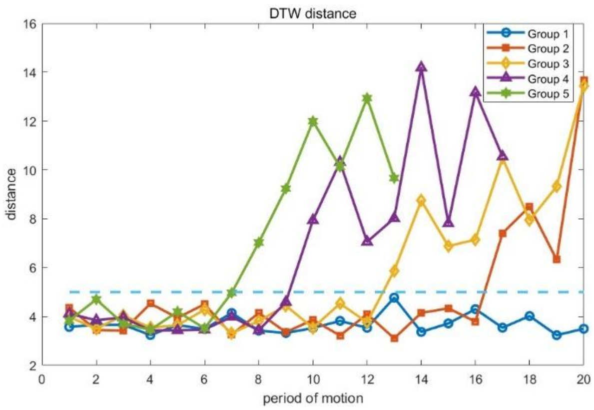

Figure 8. Results of muscle fatigue determination.

Therefore, the energy recovery rates for each set were 42.847%, 42.787%, and 42.200%, respectively. The average energy recovery rate across all sets was 41.242 ± 1.374%, resulting in a coefficient variation of 3.33% for the average energy recovery rate of all subjects with consistency. The results suggested that, for non-professional fitness enthusiasts, muscle energy recovery within 120 s accounted for approximately 41.707 ± 1.875% of the maximum muscle energy output.

Derivation of training strategies based on energy analysis

The study calculated each subject's muscle energy output and recovery during exercise to failure, along with muscle energy recovery over a 120 s rest period using the average muscle energy output of a single exercise cycle during the non-deep fatigue phase as a standard value. The results were analyzed alongside muscle recovery and maximum energy output to determine the number of dumbbell curl cycles performed during the non-deep fatigue phase, supported by the energy recovered within 120 s as follows.

$$K_{NF} = \left\lfloor \frac{\overline{Q}}{p_{\pi/2} / N} \right\rfloor \tag{18}$$

The number of dumbbell curl cycles in the non-deep fatigue phase was represented by N, while K_{NF} represented the number of curls muscles performed during the non-deep fatigue stage, supported by energy restored during a 120 s rest period. K_{NF} played a pivotal role in assessing individual exercise capacity and quantitatively planning dumbbell curl cycles. The study further derived two exercise strategies to guide practical training, which were not predefined experimental protocols, but rather practical recommendations based on experimental results, aimed at improving training efficiency and reducing the risk of injury while ensuring muscles not reaching a state of deep fatigue. The strategy 1 was that energy production during muscle contraction continued until reaching the threshold between non-deep and deep fatigue states. From the second to the fifth set, the energy output of each set remained matching to the energy recovered during the 120 s rest intervals. This strategy maximized training efficiency, ensured muscle safety, and promoted muscle tissue growth. Strategy 2 was performing five consecutive sets of dumbbell curls with the energy output of each set equivalent to the energy recovered during 120 seconds of rest. This plan ensured sustainable performance over time, maintained muscle endurance, and maximized comfort. In addition, to illustrate the impact of energy imbalance on muscle condition, this study constructed a non-recommended scenario for comparative analysis, which was strategy 3 that three consecutive sets of dumbbell curls were performed with 22 repetitions per set, ensuring that the energy expenditure exceeded the amount recoverable within a 120 s rest interval. This plan was served as the control group, demonstrating that an unscientific exercise plan induced deep muscle fatigue. The results showed that, under strategies 1 and 2, which were derived based on energy balance, the DTW distance between the angular velocity of each exercise cycle and the reference angular velocity was less than 5, indicating that the muscles remained in a non-deep fatigue state throughout the entire exercise. In contrast, in strategy 3 where energy expenditure exceeded the recovery capacity within 120 seconds, the DTW

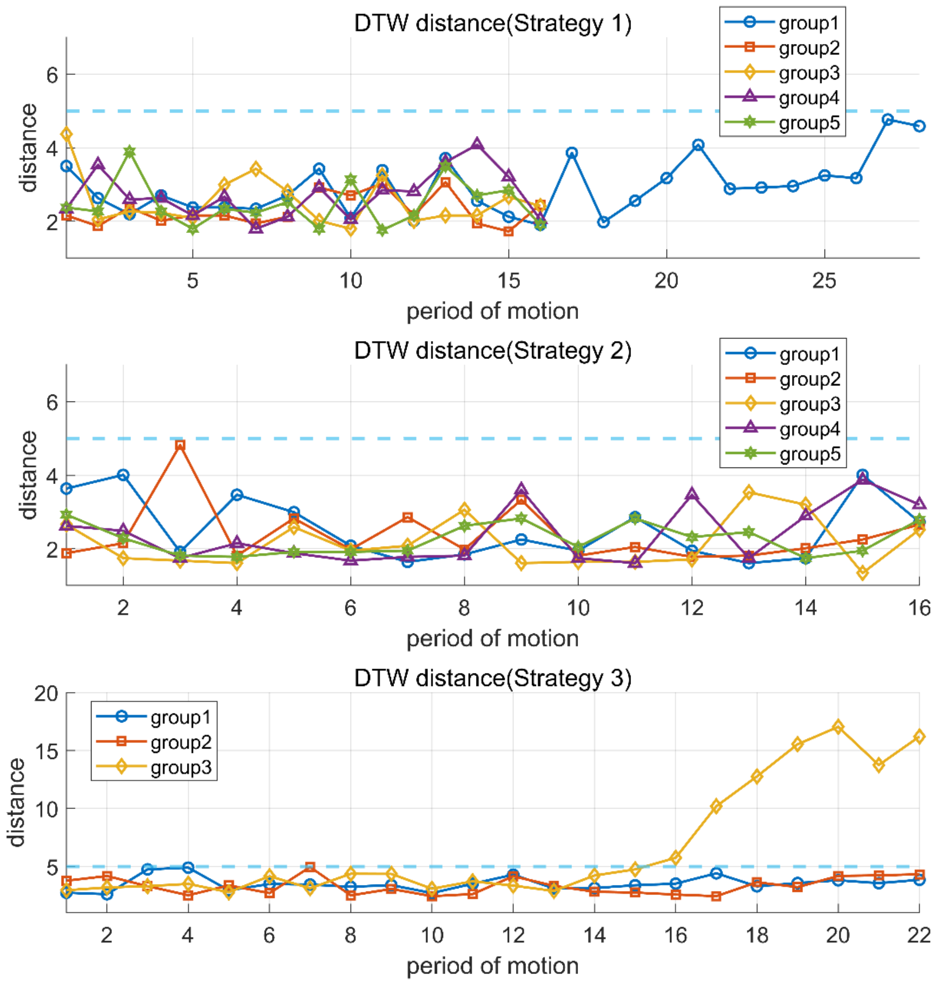

Figure 9. Fatigue assessment results under different training strategies derived from the energy ratio parameter *K*. Strategies 1 and 2 maintained a balance between energy expenditure and recovery, preventing deep fatigue. Strategy 3 exceeded the recoverable energy threshold and led to deep fatigue.

distance exceeded 5 in some exercise cycles, suggesting that, as exercise progressed, the muscles gradually entered a state of deep fatigue, and continuing the exercise might increase the risk of muscle injury (Figure 9). The results demonstrated that training strategies based on energy balance enabled sustainable muscle exercise and effectively prevented the onset of deep fatigue, which was of great significance for ensuring the safety and feasibility of the exercise process.

Evaluation of different participants

Fatigue analysis based on energy output was compared with rapid refined composite multiscale sample entropy (R2CMSE) method [27]. R2CMSE was employed to enhance conventional multiscale sample entropy analysis. These approaches were applied to examine randomly selected 90 dumbbell curl exercises. R2CMSE was based on multiscale entropy (MSE) and composite multiscale entropy (CMSE) algorithms. It not only enhanced the complexity estimation of timing signal complexity but also reduced the uncertainty entropy [28]. The analysis showed that the R2CMSE feature values from the electromyography signal tended to decrease overall with the increase of muscle fatigue. However, R2CMSE eigenvalues were not strictly monotonically decreasing but exhibited an overall downward trend with localized irregularities. The movement deviation boundary line was derived by linearly fitting a dataset of feature signals in conjunction with angular velocity analysis utilizing the DTW algorithm. This boundary line was employed to predict fatigue states, specifically, feature values situated above the boundary line indicated a state of non-deep fatigue, whereas those situated below it indicated a state of deep fatigue. The results showed that the irregular feature value points above and below the movement deviation boundary line demonstrated a maximum adjacent difference of 0.42. In the deep fatigue phase (gray area), multiple feature values were above the movement deviation boundary line. On the contrary, in the non-deep fatigue (white area), multiple feature values dropped below the line (Figure 10). Therefore, this method was not suitable for distinguishing the deep fatigue stage.

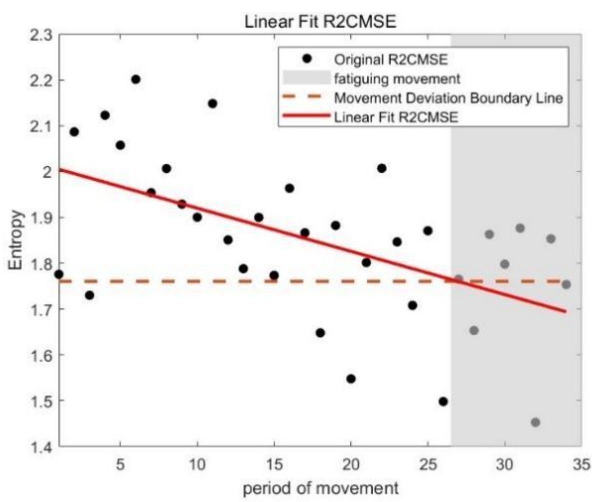

Figure 10. Analysis results of R2CMSE.

This study analyzed the entire movement process based on muscle energy output. The predicted moments of deep fatigue zone accounting for 72.782 ± 2.702% and derived from the analysis of $p_{\pi/2}$ values across all participants served as the predictive range for determining the critical point of muscle deep fatigue. The movements before and after the deep fatigue critical point were effectively differentiated by the muscle fatigue assessment method based on energy output. The results of prediction were consistent with the actual outcomes, which were represented by the gray areas (Figure 11).

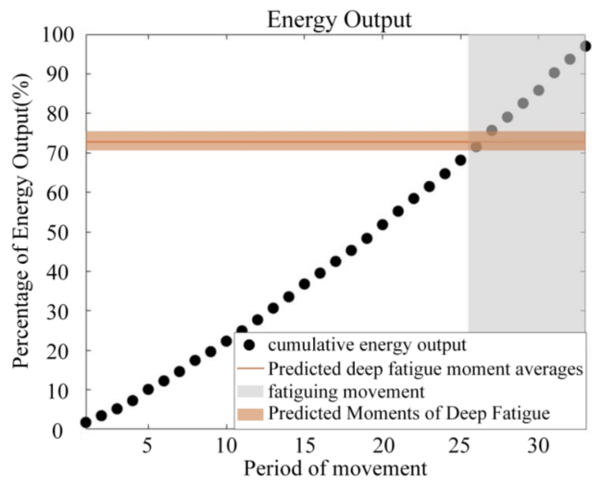

Figure 11. Prediction based on the energy output method.

Conclusion

In this study, DTW was utilized to analyze angular velocity signals from elbow joints during dumbbell curls, enabling the determination of muscle contraction intensity. Motion distortion was identified as a key indicator of deep fatigue, allowing for accurate determination of the deep fatigue threshold. The Hill model-based muscle energy output calculation method was adopted to investigate the deep and non-deep fatigue stages to accurately predict deep fatigue status. The results indicated that movement distortion preceded task failure, suggesting that muscle strength had declined to a critical level, specifically, below that required to achieve optimal contraction, ultimately leading to deep muscle fatigue. The muscle contraction energy was quantified through the Hill model, and when the energy out reached 72.78 ± 2.70% of maximum output, the muscle was in a deep fatigue state. The muscle recovery energy within a 120 second rest period was 41.71 ± 1.88% of the maximum output energy, which validated that this study established a scientific standard for personalized exercise planning. Given the differences in exercise and individuals, more research is needed on the quantitative energetic characteristics of muscle fatigue. Future studies should comprehensively account for exercise-related variables with a focus on quantifying muscle energy output profiles and their relationship with fatigue under varying loads and across diverse populations.

Acknowledgements

This research was partially supported by Natural Science Foundation Project of Hebei, China (Grant No. C2024203005), Major Project of Basic Science Research of Jiangsu Province Universities, China (Grant No. 23KJA460012), and Initial Scientific Research Fund Project of Suzhou Vocational Institute of Industrial Technology, China (Grant No. 2017kyqd022).

References

1. Shariatzadeh M, Hafshejani EH, Mitchell CJ, Chiao M, Grecov D. 2023. Predicting muscle fatigue during dynamic contractions using wavelet analysis of surface electromyography signal. Biocybern Biomed Eng. 43(2):428-441.
2. Aghdam SR, Alizadeh SS, Rasoulzadeh Y, Safaiyan A. 2019. Fatigue assessment scales: A comprehensive literature review. Arch Hyg Sci. 8(3):145.
3. Montull L, Vázquez P, Hristovski R, Balagué N. 2020. Hysteresis behaviour of psychobiological variables during exercise. Psychol Sport Exerc. 48:101647.
4. Scano A, Pirovano I, Manunza ME, Spinelli L, Contini D, Torricelli A, *et al*. 2020. Sustained fatigue assessment during isometric exercises with time-domain near infrared spectroscopy and surface electromyography signals. Biomed Opt Express. 11(12):7357-7375,
5. Sun J, Liu G, Sun Y, Lin K, Zhou Z, Cai J. 2022. Application of surface electromyography in exercise fatigue: A review. Front Syst Neurosci. 16:893275.
6. Wu SD, Wu CW, Lin SG, Lee KY, Peng CK. 2014. Analysis of complex time series using refined composite multiscale entropy. Phys Lett A. 378(20):1369-1374.
7. Lee YJ, Wei MY, Chen YJ. 2022. Multiple inertial measurement unit combination and location for recognizing general, fatigue, and simulated-fatigue gait. Gait Posture. 96:330-337.
8. Ameli S, Naghdy F, Stirling D, Naghdy G, Aghmesheh M. 2015. Assessment of exercise induced fatigue through motion analysis. TENCON 2015 - 2015 IEEE Region 10 Conference, Macao, China. 2015:1-4,
9. Mu D, Li F, Yu L, Du C, Ge L, Sun T. 2022. Study on exercise muscle fatigue based on sEMG and ECG data fusion and temporal convolutional network. Plos One. 17(12):e0276921.
10. Ai Q, Zhang Y, Qi W, Liu Q, Chen K. 2017. Research on lower limb motion recognition based on fusion of sEMG and accelerometer signals. Symmetry. 9(8):147.
11. Westerblad H, Allen DG, Lannergren J. 2002. Muscle fatigue: lactic acid or inorganic phosphate the major cause? Physiology. 17(1):17-21.
12. Kabbara AA, Allen DG. 2001. The use of the indicator fluo-5N to measure sarcoplasmic reticulum calcium in single muscle fibres of the cane toad. J Physiol. 534(Pt 1):87-97.
13. Lännergren J, Bruton JD, Westerblad H. 2000. Vacuole formation in fatigued skeletal muscle fibres from frog and mouse: Effects of extracellular lactate. J Physiol. 526(3):597-611.
14. Marco G, Alberto B, Taian V. 2017. Surface EMG and muscle fatigue: Multi-channel approaches to the study of myoelectric manifestations of muscle fatigue. Physiol. Meas. 38(5):R27.
15. Allen DG, Lamb GD, Westerblad H. 2008. Skeletal muscle fatigue: Cellular mechanisms. Physiol Rev. 80(1):287-332.
16. Braithwaite B, Plamondon R, Begon M. 2020. Muscle activation profiles based on the proportionality hypothesis of the kinematic theory of human movements. 2020 17th International Conference on Frontiers in Handwriting Recognition (ICFHR), Dortmund, Germany. 2020:331-336.
17. Desplenter T, Trejos AL. 2018. Evaluating muscle activation models for elbow motion estimation. Sensors. 18(4):1004.
18. Moussa EM, Lelore T, Mouchère H. 2023. Point to segment distance DTW for online handwriting signals matching. 12th International Conference on Pattern Recognition Applications and Methods. 2023:850-855.
19. Amin TB, Mahmood I. 2008. Speech recognition using dynamic time warping. 2008 2nd International Conference on Advances in Space Technologies, Islamabad, Pakistan. 2008:74-79.
20. Permanasari Y, Harahap EH, Ali EP. 2019. Speech recognition using dynamic time warping (DTW). J Phys Conf Ser. 1366(1):012091.
21. Göktepe S, Menzel A, Kuhl E. 2014. The generalized Hill model: A kinematic approach towards active muscle contraction. J Mech Phys Solids. 72:20-39.
22. Sawicki GS, Khan NS. 2016. A simple model to estimate plantar flexor muscle-tendon mechanics and energetics during walking with elastic ankle exoskeletons. IEEE Trans Biomed Eng. 63(5):914-923.
23. Alexander RM. 1997. Optimum muscle design for oscillatory movements. J Theor Biol. 184(3):253-259.
24. Arnold EM, Delp SL. 2011. Fibre operating lengths of human lower limb muscles during walking. Philos Trans R Soc Lond B Biol Sci. 366(1570):1530-1539.
25. Lee HS. 2019. Application of dynamic time warping algorithm for pattern similarity of gait. J Exerc Rehabil. 15(4):526.
26. Ramos JS, Dalleck LC, Tjonna AE, Beetham KS, Coombes JS. 2015. The impact of high-intensity interval training versus

moderate-intensity continuous training on vascular function: A systematic review and meta-analysis. Sports Med. 45:679-692.

27. Wang S, Tang H, Wang B, Mo J. 2021. Analysis of fatigue in the biceps brachii by using rapid refined composite multiscale sample entropy. Biomed Signal Process Control. 67:102510.
28. Wu SD, Wu CW, Lin SG, Lee KY, Peng CK. 2014. Analysis of complex time series using refined composite multiscale entropy. Phys Lett A. 378(20):1369-1374.